Short Communication

Simulations reveal causes of inter-regional differences in Pliocene climatic periodicity

Xiaofang Huang[a*], Shiling Yang[a, b*], Alan Haywood[c], Julia Tindall[c], Dabang Jiang[d, b], Yongda Wang[a], Minmin Sun[a, b], Shihao Zhang[a, b], Zhongli Ding[a]

[a]Key Laboratory of Cenozoic Geology and Environment, Institute of Geology and Geophysics, Chinese Academy of Sciences, Beijing 100029, China

[b]College of Earth and Planetary Sciences, University of Chinese Academy of Sciences, Beijing 100049, China

[c]School of Earth and Environment, University of Leeds, Leeds LS2 9JT, UK

[d]Institute of Atmospheric Physics, Chinese Academy of Sciences, Beijing 100029, China

*Correspondence to: Xiaofang Huang, hxf@mail.iggcas.ac.cn

Shiling Yang, yangsl@mail.iggcas.ac.cn

Received 2022-09-07，Revised 2022-11-03，accepted 2022-11-04

The Pliocene Epoch (5.33 to 2.58 Ma) is the last period of sustained warmth before the emergence of the large-scale Pleistocene glaciations. This period was generally warm and wet and is often used as an analogue for near-future climate conditions in terms of CO_2 levels (~400 ppm, 1 ppm=1 μmol/mol), and comparable temperatures. Evaluating the climate system and its fluctuation patterns during the Pliocene warm period provide scientists with the opportunity to understand a warmer-than-present world, and are fundamental to our understanding and ability to accurately project future climate and environmental change.

During the Pliocene, a dominant obliquity cycle (41 ka) was identified from marine δ^{18}O-based global ice volume reconstructions and high-latitude continental records (Fig. 1; e.g., [1]). In contrast, dust and pollen records from low latitudes and the Mediterranean region show a dominance of the precession cycle (21 ka) (Fig. 1; e.g., [2]), and proxy records derived from aeolian deposition in the mid-latitude monsoonal Asia display a mix of precession, obliquity, and eccentricity (100 ka) cycles (Fig.1; e.g., [3]). However, the underlying mechanisms for these inter-regional differences in climatic cycles remain to be clarified.

Numerical experiments have emerged as an efficient means of understanding past climate over regional and global scales, and have been used to explore the process and mechanism of Pliocene climate change [4]. Therefore, the dominant orbital parameter drivers of the Pliocene climate variability can be studied using simulations. In this study, we designed sensitivity experiments using a coupled climate model to explore the effect of changes in orbital parameters on climate during the Pliocene, with the aim of investigating the mechanism of inter-regional differences in climatic periodicity.

The Hadley Centre coupled climate model version 3 (hereafter referred to as HadCM3) was used for this study. Model description and detail boundary conditions can be found in the supplementary material. Our simulations are based on Bragg et al. [5] but used the MOSES 2 surface exchange scheme as described in Tindall et al. [6]. The other one difference between our simulations and Bragg's PlioMIP1 simulation is that we use different orbital parameters than those applied in the PlioMIP1 simulation which assigns modern orbital configuration [5].

We perform a set of idealized sensitivity experiments (Table 1) to isolate the effect of variations in obliquity, precession, and eccentricity on climate during the mid-Pliocene warm period. In briefly, the suite includes (1) maximum eccentricity, maximum precession, and minimum obliquity (hereafter $E_{\max}P_{\max}O_{\min}$), (2) maximum eccentricity, minimum precession, and minimum obliquity (hereafter $E_{\max}P_{\min}O_{\min}$), (3) maximum eccentricity, maximum precession, and maximum obliquity (hereafter $E_{\max}P_{\max}O_{\max}$), and (4) minimum eccentricity, maximum precession, and minimum obliquity (hereafter $E_{\min}P_{\max}O_{\min}$). These eccentricity, obliquity and precession values represent the extremes of their theoretical orbital variations obtained from Laskar et al. [7] during the mid-Pliocene warm period. Except the orbital parameters, all other boundary conditions in the sensitivity experiments are the same.

All experiments started from the end of the HadCM3 PlioMIP1 simulation, and continued for another 160 ($E_{max}P_{max}O_{min}$), 150 ($E_{max}P_{min}O_{min}$), 240 ($E_{max}P_{max}O_{max}$), and 200 ($E_{min}P_{max}O_{min}$) model years until the model climate equilibrated to the boundary conditions. Climate statistics are based on time averages of the final 30 years for each run. The results are presented as anomalies between the sensitivity experiments of the extremes of each orbital parameter, thereby allowing estimation each orbital parameter's effect on climate during the mid-Pliocene warm period.

Table 1 Experimental design for the orbital extreme sensitivity experiments

Experiment name	Eccentricity (*E*)	Precession (*P*)	Obliquity (*O*)	Boundary conditions	Years for analysis
$E_{max}P_{max}O_{min}$	0.0607	Perihelion	22°	PRISM3D	30
$E_{max}P_{min}O_{min}$	0.0607	Aphelion	22°	PRISM3D	30
$E_{max}P_{max}O_{max}$	0.0607	Perihelion	24.5°	PRISM3D	30
$E_{min}P_{max}O_{min}$	0.005	Perihelion	22°	PRISM3D	30

The effects of a change in Earth's obliquity (axial tilt) can be physically interpreted as a redistribution of the insolation by changing its meridional gradient, but at the same time keeping the total solar radiation incident upon the Earth the same [8]. An increase in the obliquity from 22.0° to 24.5° raises the annual mean air temperature (MAT) over most areas of the globe (Fig. 2a) but induces a small decrease at the equator (~1 °C). The corresponding zonally averaged annual MAT show a significant increase at high latitudes by more than 5 °C and a slight change by 0−1 °C at the equator (Fig. 2b), which is consistent with the insolation changes (Fig. S1). The simulated annual MAT between precession minimum and maximum shows slight differences in most areas (~±2 °C; Fig. 2c), and the corresponding zonally averaged annual MAT also shows a small change (±1.5 °C) at most latitudes (Fig. 2d). For variation in eccentricity, the simulated annual MAT results demonstrate nearly pervasive warming over the globe (~1−3 °C; Fig. 2e), with an ~2.5 °C increase in zonally averaged annual MAT at high latitudes and a warming of ~1 °C at low latitudes (Fig. 2f). Clearly, Variations in the Earth's orbital parameters (obliquity, precession, and eccentricity) during the mid-Pliocene warm period have small effect on the annual MAT consistently at most low latitudes, while obliquity change has the most effect on the annual MAT at high latitudes.

The shift in obliquity from minimum to maximum values leads to a small increase in mean annual precipitation (MAP; ~0.5 mm d^{-1}) over most areas of the globe (Fig. 2g) and a small decrease in MAP (~–1 to 0 mm d^{-1}) at the equator (Fig. 2g, h). The change in precession from aphelion to perihelion results in greatest enhancement (~1.5–3 mm d^{-1}) and deficit (~–2 mm d^{-1}) in MAP at low latitudes, associated with small precipitation changes at high latitudes (Fig. 2i, j). The eccentricity extreme-value experiments (Fig. 2k) show a spatial MAP pattern similar to that observed in the obliquity experiments (Fig. 2g); i.e., a small precipitation change (~0.5 mm d^{-1}) over the globe except a larger magnitude of change at low latitudes (~±1.5 mm d^{-1}; Fig. 2l). Evidently, changes in the values of Earth's orbital parameters (obliquity, precession, and eccentricity) during the mid-Pliocene warm period have small effect on the MAP consistently at high latitudes, while precession change has the most effect on the MAP at low latitudes.

Climatic periodicity during the Pliocene has been studied extensively using various proxies, enabling us to assemble a dataset that can be used to analyze global climatic periodicity during the Pliocene (Fig. 1 and Table S1 online). This dataset contains 76 records (Table S1 online), of which 24, 22, and 6 show a dominance of obliquity, precession, and eccentricity, respectively. The remaining records display a mixed signal of the two (17 records) or three (7 records) of the astronomical parameters.

High-latitude terrestrial records and the deep-sea δ^{18}O records, which are influenced mainly by ice volume at both northern and southern high latitudes [9], exhibit a 41-ka cycle [1]. Our simulation results show that obliquity change has the greatest effect on the high-latitude temperature, highlighting the strong influence of obliquity on high-latitude ice volume, which is consistent with geological records (Fig. 1) and previous simulations [8]. It should be noted that some low-latitude deep-sea δ^{18}O records also reveal a dominance of the obliquity cycle, as the abundances of ^{18}O and ^{16}O in the ocean water are uniformly controlled by high-latitude ice volume.

Low-latitude and Mediterranean records, such as dust, pollen, Mediterranean sapropel formation and lake levels (Fig. 1; e.g., [2]), appear to be directly linked to monsoonal variations, showing a predominant 21 ka precession period. These records are consistent with our simulated results and previous simulations [10], which show that precession change has the most effect on the low-latitude precipitation. The precession variations affect monsoon by changing the seasonal solar radiation at the top of the atmosphere, thereby influencing the regional hydrological cycle. Of particular note is that Mediterranean $\delta^{18}O$ records also reveal a clear precession cycle (Fig. 1; e.g., [11]), which differs from the dominant obliquity cycle in other deep-sea $\delta^{18}O$ records (Fig. 1; e.g., [1]). This may result from the combined effect of the semi-isolated nature of the Mediterranean Sea and the rate of evaporation controlled by precession-modulated low-latitude insolation.

It is striking that the geological records from the Chinese Loess Plateau display a mix of astronomical signals (Fig. 1). Numerous studies have demonstrated that the dust of the Loess Plateau is transported by the East Asian winter monsoon, while the soil formation and biological processes are controlled by the East Asian summer monsoon (e.g., [12]). The winter monsoon intensity is closely related to ice volume oscillations at high northern latitudes [13], and the summer monsoon is directly linked to precession variations [14]. Our simulations show that obliquity and precession have the most effect on the high-latitude temperature and low-latitude precipitation, respectively (Fig. 2a, i), which well explain the mix of precession and obliquity signals over the Chinese Loess Plateau.

It should be pointed out that during the Pliocene warm period, the occurrence of the eccentricity cycle (100 ka), which has dominated the loess and ocean records since the Middle Pleistocene transition [15], is hard to be explained by the simulation results. Previous studies have interpreted the eccentricity signal in loess as a result of the asymmetric response to insolation forcing [3]; this issue will require systematic future investigation based on reconstructions and simulations.

In conclusion, the sensitivity of the climate to the extreme value of the orbital parameters during the mid-Pliocene warm period was investigated using the HadCM3 model. Results show that the temperature changes induced by obliquity are >5 °C over high latitudes and ~0–2 °C over low latitudes, while those induced by precession or eccentricity are ~0–3 °C over high latitudes and ~0–2 °C over low latitudes. In contrast, precipitation changes driven by obliquity, precession, and eccentricity are consistently very small over high latitudes, while over low latitudes, the precession induced precipitation changes are dramatic (>2 mm d^{-1}) and those induced by obliquity or eccentricity are ~0–1 mm d^{-1}. Our results show that the most notable effect of obliquity on climate occurs at high latitudes, whereas precession affects the climate mainly over low latitudes. This well explains the regional differences in climatic periodicity during the Pliocene: the predominant 41 ka climatic periodicity at high latitudes and in marine oxygen isotope records regulated by high-latitude ice volume, and the dominant 21 ka climatic cycle over low latitudes and the Mediterranean region.

Conflict of interest

The authors declare that they have no conflict of interest.

Acknowledgments

This work was supported by the National Natural Science Foundation of China (41725010 and 42107472), the Strategic Priority Research Program of Chinese Academy of Sciences (XDB26000000 and XDB31000000), and the Key Research Program of the Institute of Geology & Geophysics, Chinese Academy of Sciences (IGGCAS-201905). We thank three anonymous reviewers for critical comments.

Author contributions

Xiaofang Huang, Shiling Yang, and Zhongli Ding designed the study; Xiaofang Huang performed the analysis and wrote the draft; Yongda Wang, Minmin Sun, and Shihao Zhang took part in the investigation; Xiaofang Huang, Alan Haywood, and Julia Tindall designed the experiment; Shiling Yang and Zhongli Ding supervised the project; Shiling Yang, Alan Haywood, Julia Tindall, Dabang Jiang revised the manuscript.

Supporting Information:

Supporting information table S1

References

[1] Drury AJ, John CM, Shevenell AE. Evaluating climatic response to external radiative forcing during the late Miocene to early Pliocene: new perspectives from eastern equatorial Pacific (IODP U1338) and North Atlantic (ODP 982) locations. Paleoceanography 2016; 31: 167–184.

[2] Grant KM, Rohling EJ, Westerhold T, et al. A 3 million year index for North African humidity/aridity and the implication of potential pan-African humid periods. Quat Sci Rev 2017; 171: 100–118.

[3] Sun Y, Clemens SC, An Z, et al. Astronomical timescale and palaeoclimatic implication of stacked 3.6-Myr monsoon records from the Chinese Loess Plateau. Quat Sci Rev 2006; 25: 33–48.

[4] Zhang R, Jiang DB, Zhang Z, et al. Modeling the late Pliocene global monsoon response to individual boundary conditions. Clim Dynam 2019; 53: 4871–4886.

[5] Bragg FJ, Lunt DJ, Haywood AM. Mid-Pliocene climate modelled using the UK Hadley Centre Model: PlioMIP Experiments 1 and 2. Geosci Model Dev 2012; 5: 1109–1125.

[6] Tindall JC, Haywood AM, Howell FW. Accounting for centennial-scale variability when detecting changes in ENSO: a study of the Pliocene. Paleoceanography 2016; 31: 1330–1349.

[7] Laskar J, Robutel P, Joutel F, et al. A long-term numerical solution for the insolation quantities of the Earth. Astron Astrophys 2004; 428: 261–285.

[8] Mantsis DF, Clement AC, Broccoli AJ, et al. Climate feedbacks in response to changes in obliquity. J Clim 2011; 24: 2830–2845.

[9] De Schepper S, Gibbard PL, Salzmann U, et al. A global synthesis of the marine and terrestrial evidence for glaciation during the Pliocene Epoch. Earth-Sci Rev 2014; 135: 83–102.

[10] Lamy F, Chiang JC, Martínez-Méndez G, et al. Precession modulation of the South Pacific westerly wind belt over the past million years. Proc Natl Acad Sci USA 2019; 116: 23455–23460.

[11] Steenbrink J, Hilgen FJ, Krijgsman W, et al. Late Miocene to Early Pliocene depositional history of the intramontane Florina-Ptolemais-Servia Basin, NW Greece: interplay between orbital forcing and tectonics. Palaeogeogr Palaeoclimatol Palaeoecol 2006; 238: 151–178.

[12] Ding ZL, Derbyshire E, Yang SL, et al. Stacked 2.6-Ma grain size record from the Chinese loess based on five sections and correlation with the deep-sea $\delta^{18}O$ record. Paleoceanography 2002; 17: 5–1.

[13] Ding ZL, Liu T, Rutter NW, et al. Ice-volume forcing of East Asian winter monsoon variations in the past 800,000 years. Quat Res 1995; 44: 149–159.

[14] Wang PX. Global monsoon in a geological perspective. Chin Sci Bull 2009; 54: 1113–1136.

[15] Wennrich V, Minyuk PS, Borkhodoev V, et al. Pliocene to Pleistocene climate and environmental history of Lake El'gygytgyn, Far East Russian Arctic, based on high-resolution inorganic geochemistry data. Clim Past 2014; 10: 1381–1399.

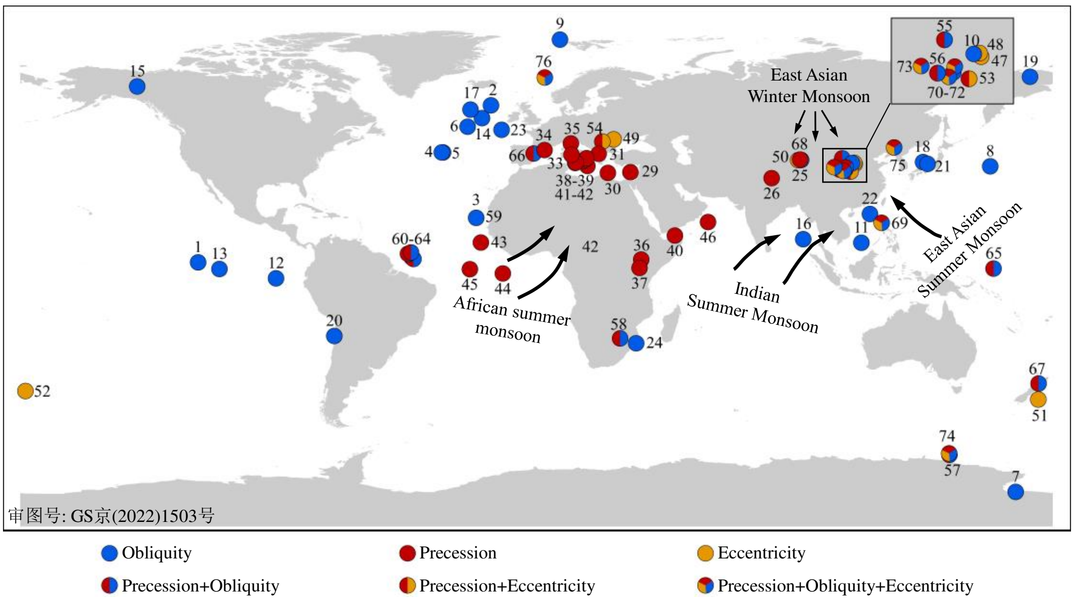

Fig. 1. Paleoclimatic records for the climatic periodicity during the mid-Pliocene.

Numbers refer to sites listed in supplementary Table S1 (online). Circles with different colors represent different astronomical signals (see legend). Circles with two or three colors denote a mixed signal of two or three orbital parameters, respectively.

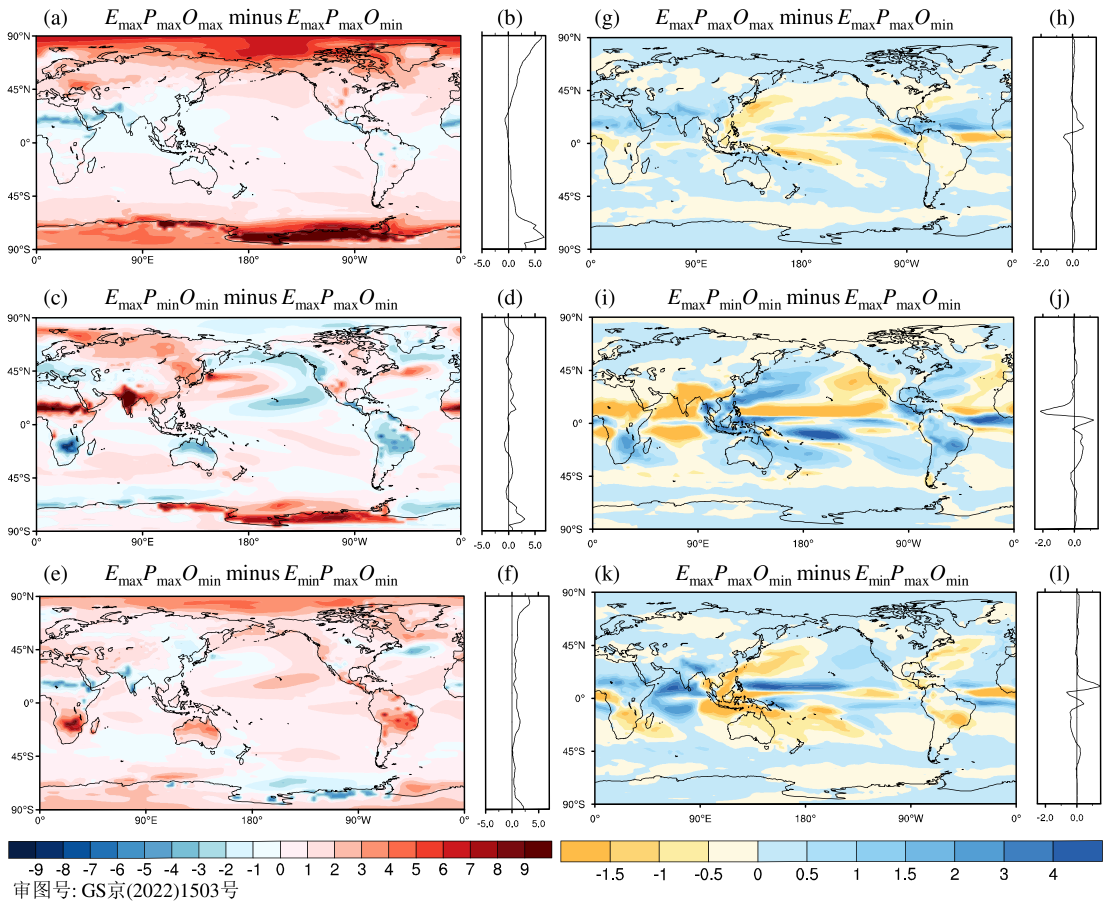

审图号: GS京(2022)1503号

Fig. 2. Annual mean surface air temperature (units: °C) and precipitation anomalies (units: mm d^{-1}) between the obliquity maximum and minimum (a, g); the precession maximum and minimum (c, i); and the eccentricity maximum and minimum variations during the mid-Pliocene warm period (e, k). Zonally averaged temperature (b, d, f) and precipitation (h, j, l) changes are plotted in the side panels.